

***New Phytologist* Supporting Information**

Article title: Common mechanisms explain nitrogen-dependent growth of Arctic shrubs over three decades despite heterogeneous trends and declines in soil nitrogen availability

Authors: Andrew C. Martin, Marc Macias-Fauria, Michael B. Bonsall, Bruce Forbes, Pentti Zetterberg, and Elizabeth S. Jeffers

Article acceptance date: [Click here to enter a date.](#)

The following Supporting Information is available for this article:

Fig. S1 Wood N Concentration

Fig. S2 Yuribei Ring Width Chronology

Fig. S3 Expected growth trajectories given best-fitting parameters

Table S1 Summary statistics for individual $\delta^{15}\text{N}$ time-series

Table S2 Parameter bounds from which starting values were drawn

Table S3 Root mean square error (RMSE) values for ring width (mm) given one-step-ahead predictions of shrub-nitrogen relations

Table S4 Root mean square error (RMSE) values for $\delta^{15}\text{N}$ (‰) given one-step-ahead predictions of shrub-nitrogen relations

Table S5 Minimum -log Likelihood value for model fits

Methods S1 Ring width chronology development

Methods S2 Creation of wood thin section cutting guides

Methods S3 Simulated annealing implementation

Methods S4 Bristlecone Model script for model-fitting and model-selection

Note S1 Sensitivity analysis of a global versus local calibration of the $\delta^{15}\text{N}$ – N relationship

Fig. S1 Percentage nitrogen concentration (%N) time-series for ten shrub individuals at Yuribei.

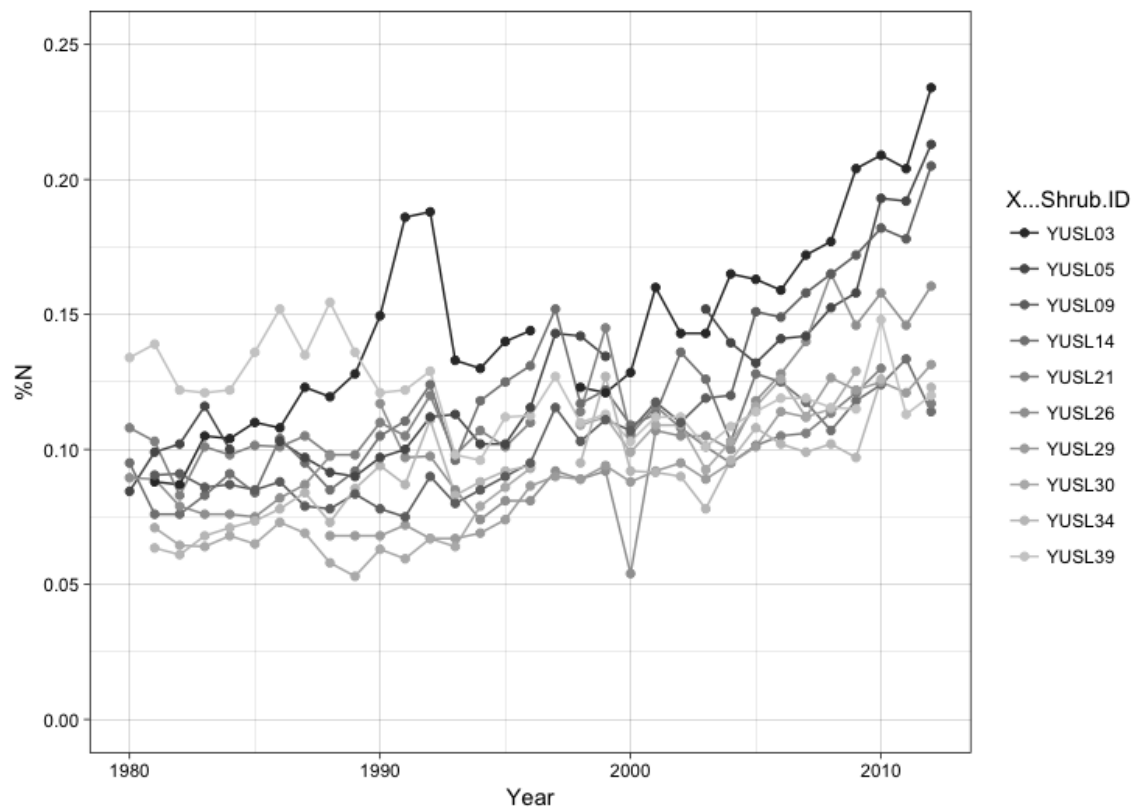


Fig. S2 Mean ring width chronology for Yuribei developed from 52 shrub disc ring width measurements. Tukey's biweight robust mean was applied to all 52 raw measurement (not detrended) ring width time-series resulting in a mean chronology. Sample Depth indicates the number of increments contributing to the mean of each year respectively.

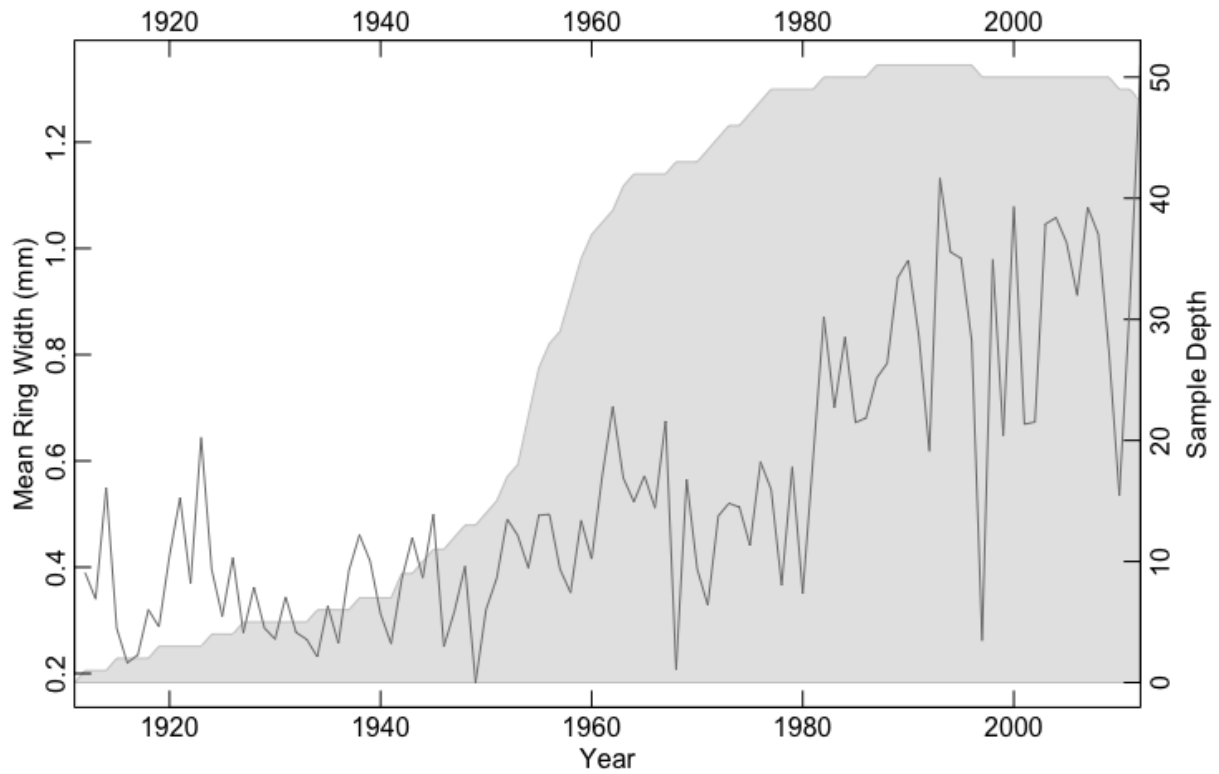


Fig. S3 Expected growth trajectories for each plant and hypothesis given the best-fitting parameters. Actual measurements are represented by black points.

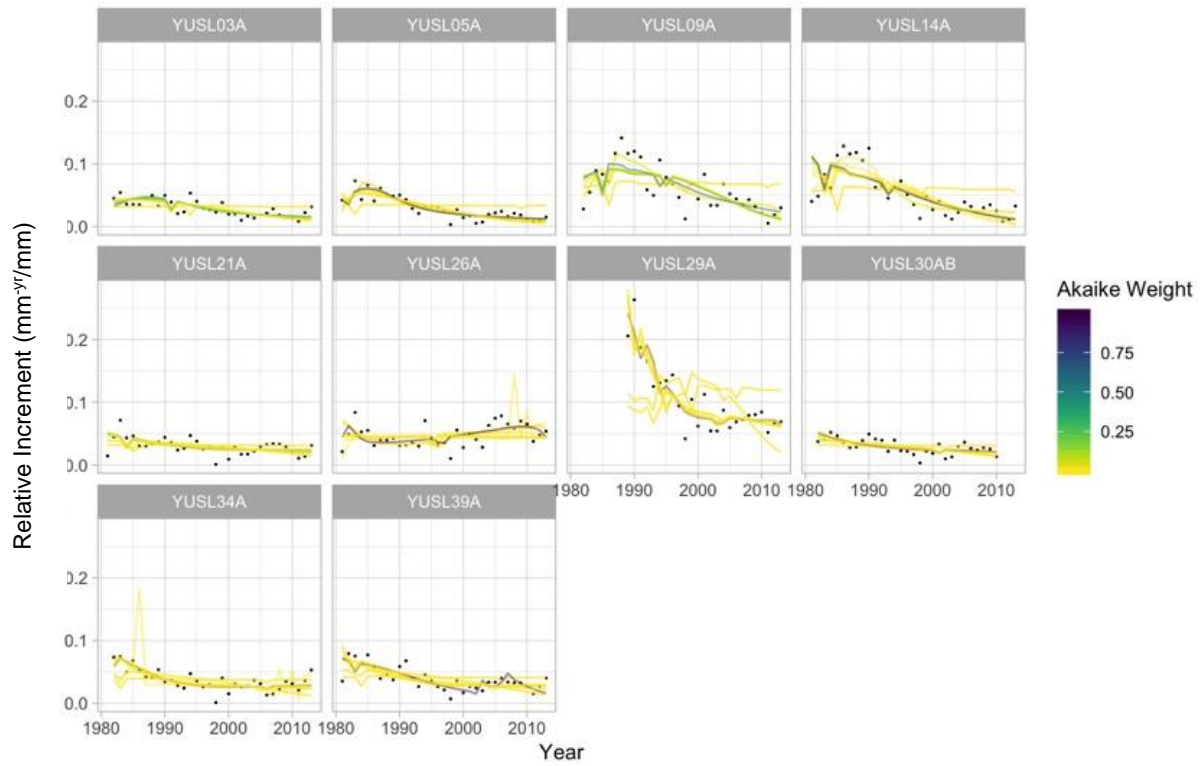


Table S1 Summary statistics for individual $\delta^{15}\text{N}$ time-series

Shrub Individual	Mean $\delta^{15}\text{N}$	Standard Deviation $\delta^{15}\text{N}$
YUSL3	0.719	0.57496399
YUSL5	0.478684211	0.616214121
YUSL9	0.211428571	0.439476248
YUSL21	-1.116666667	0.325853804
YUSL26	-1.623333333	1.002517968
YUSL29	-1.647179487	0.56582473
YUSL30	-1.802	0.559662714
YUSL14	-1.880714286	0.485704883
YUSL34	-1.989	0.602187465
YUSL39	-2.833809524	0.687824256

Table S2 Parameter bounds from which starting values were drawn for each model-fitting procedure.

Parameter	Constraint	Lower Bound	Upper Bound
λ	Positive only	0.001	0.500
γ_N	Positive only	0.001	0.200
γ_B	Positive only	0.001	0.200
ρ	Unconstrained	-0.500	0.500
σ_x	Positive only	0.001	0.100
σ_y	Positive only	0.001	0.100
K	Positive only	3000	5000
α	Positive only	0.0001	0.010
a	Positive only	1.000×10^{-4}	4.000×10^{-4}
h	Positive only	0.100	0.400
r	Positive only	0.100	1.000

Starting values were drawn from a uniform distribution between the lower and upper bound.

During the model-fitting procedure, it was illegal for parameter estimates to invalidate any specified constraints above (e.g., illegal to have a negative value when specified to be positive only); parameter values, however, were otherwise unrestricted and could optimise to any numeric value.

Table S3 Root mean square error (RMSE) values for ring width (mm) given one-step-ahead predictions of shrub-nitrogen relations

Shrub ID:	03A	05A	09A	14A	21A	26A	29A	30AB	34A	39A
<i>Non-Asymptotic</i>										
Saturating	0.19	0.31	0.64	0.52	0.35	0.38	1.16	0.47	1.25	13.78
Saturating + Feedback	0.20	0.45	0.96	0.69	0.31	0.80	0.91	0.78	0.94	1.48
Linear	0.18	0.31	0.56	0.51	0.34	1.02	1.21	0.75	1.03	1.57
Linear + Feedback	0.20	0.48	0.87	0.86	0.31	0.92	0.81	0.77	1.05	1.08
No N Limitation	0.28	0.51	0.83	0.74	0.31	0.35	0.83	0.40	0.45	0.50
Plant-Driven N Cycling	0.27	0.51	0.83	0.74	0.31	0.35	0.84	0.40	0.45	0.50
<i>Asymptotic</i>										
Saturating	0.18	0.26	1.11	0.39	0.34	0.38	1.13	0.40	0.66	0.63
Saturating + Feedback	0.18	0.31	0.41	0.50	0.33	0.83	0.74	0.50	0.95	2.19
Linear	0.18	0.26	0.42	0.41	0.29	0.75	1.41	1.92	1.03	1.41
Linear + Feedback	0.18	0.32	0.99	0.35	0.28	0.88	0.91	0.56	0.91	1.07
No N Limitation	0.19	0.27	0.41	0.38	0.27	0.35	0.64	0.34	0.52	0.47
Plant-Driven N Cycling	0.19	0.27	0.41	0.40	0.27	0.35	0.64	0.34	0.52	0.47

All values shown to two decimal places.

Table S4 Root mean square error (RMSE) values for $\delta^{15}\text{N}$ (‰) given one-step-ahead predictions of shrub-nitrogen relations

Shrub ID:	03A	05A	09A	14A	21A	26A	29A	30AB	34A	39A
<i>Non-Asymptotic</i>										
Saturating	0.36	0.66	0.40	0.41	0.33	0.60	0.58	0.53	0.65	0.92
Saturating + Feedback	0.38	0.71	1.47	0.39	0.33	0.70	0.56	0.52	0.66	0.92
Linear	0.36	0.66	0.41	0.72	0.32	0.59	0.60	0.51	0.65	0.81
Linear + Feedback	0.38	0.63	1.54	0.47	0.33	0.71	1.66	0.56	0.65	0.76
No N Limitation	0.45	0.50	0.39	0.34	0.34	0.58	0.61	0.49	0.67	0.90
Plant-Driven N Cycling	0.42	0.50	0.39	0.34	0.32	0.61	0.64	0.51	0.66	0.91
<i>Asymptotic</i>										
Saturating	0.38	0.54	-	0.36	0.33	0.61	0.58	0.50	0.72	0.73
Saturating + Feedback	0.39	0.53	0.39	0.34	0.34	0.69	0.78	0.50	0.65	0.96
Linear	0.38	0.54	0.36	0.36	0.33	0.78	0.62	0.53	0.65	0.77
Linear + Feedback	0.39	0.53	0.38	0.38	0.32	0.76	0.58	0.50	0.63	0.76
No N Limitation	0.45	0.50	0.39	0.34	0.35	0.58	0.58	0.50	0.72	0.90
Plant-Driven N Cycling	0.45	0.50	0.39	0.36	0.35	0.58	0.58	0.49	0.72	0.90

All values shown to two decimal places.

Table S5 Minimum -log Likelihood value for model fits

Shrub ID:	03A	05A	09A	14A	21A	26A	29A	30AB	34A	39A
<i>Non-Asymptotic:</i>										
Saturating	46.766	85.730	90.627	81.580	52.305	114.884	41.523	86.135	75.977	92.567
Saturating + Feedback	37.026	63.471	79.178	72.890	50.801	108.664	34.483	72.889	65.646	77.850
Linear	46.029	85.728	92.903	76.308	54.206	148.435	48.593	85.492	86.800	101.710
Linear + Feedback	37.270	63.463	81.448	72.694	51.045	108.472	34.258	73.090	63.569	85.623
No N Limitation	130.517	209.118	177.561	184.782	98.494	139.626	147.033	127.110	166.107	201.781
Plant-Driven N Cycling	106.121	209.215	171.700	184.814	95.971	124.019	141.487	122.752	165.946	201.076
<i>Asymptotic:</i>										
Saturating	39.537	69.444	78.194	71.977	52.609	123.749	39.203	83.805	87.023	70.674
Saturating + Feedback	35.740	56.728	78.345	65.826	51.007	108.517	34.286	71.708	64.515	79.174
Linear	39.508	69.333	85.162	72.434	54.877	113.019	54.522	69.513	85.185	108.349
Linear + Feedback	35.916	57.084	73.637	66.207	51.817	100.556	35.414	71.728	66.835	85.801
No N Limitation	58.062	91.518	78.193	86.718	64.073	140.151	104.834	85.472	120.619	142.274
Plant-Driven N Cycling	58.101	91.717	78.217	78.539	64.097	140.029	104.846	82.174	120.656	142.255

All values shown to three decimal places.

Methods S1 Ring width chronology and percentage N data.

We did not detrend any of the measured ring width series, as they exhibited no age-related trends. We created a mean ring-width chronology using the Dendrochronology Program Library in R (Bunn 2008). Tukey's biweight robust mean was applied to all 52 raw measurement (not detrended) ring width time-series resulting in a mean chronology. All ring width data and the mean chronology will be uploaded to the International Tree Ring Database on publication. Measurements of the nitrogen concentration of wood increments (Wood [N]) were produced alongside $\delta^{15}\text{N}$. The measurements conform with other evidence that N concentrations in wood decrease from the bark inwards before stabilising, which reflects N nutrition within the plant (Gerhart & McLauchlan 2014). We did not use this data within our modelling approach, as wood [N] has not been found to record any environmental signals.

Bunn, A.G., 2008. A dendrochronology program library in R (dplR). *Dendrochronologia*, 26(2), pp.115–124.

Gerhart, L.M. & McLauchlan, K.K., 2014. Reconstructing terrestrial nutrient cycling using stable nitrogen isotopes in wood. *Biogeochemistry*, 120(1-3), pp.1–21.

Methods S2 Protocol used for creation of thin sections as cutting guides.

To create a cutting guide, a stained thin section was made from each shrub wood block. A 20µm wood thin section was taken using a microtome after wetting with de-ionised water. Thin sections were stained following standard procedures (Gärtner & Schweingruber 2013); each was washed with water, then stained for five minutes using an evenly-spread mixture of 0.5% Alcian Blue / 0.5% Safranin. Samples were then cleaned with water, 70% ethanol, 90% ethanol, dehydrated with xylene, sealed in Canada Balsam, and finally baked for 12 hours in an 80°C oven to harden. Slides were scanned at 7200dpi, and rings identified manually using Fiji image analysis software (Schindelin et al. 2012). These measurements were verified against pointer years from existing raw measurements for validation.

Gärtner, H. & Schweingruber, F.H., 2013. *Microscopic Preparation Techniques for Plant Stem Analysis*,

Schindelin, J. et al., 2012. Fiji: an open-source platform for biological-image analysis. *Nature methods*, 9(7), pp.676–682.

Methods S3 Simulating annealing implementation used for model-fitting stage.

Simulated annealing is a metaheuristic based on random walk MCMC, which mimics the physical process of annealing metal: the system is elevated to a high energy E , at which particles are likely to accept nearly all uphill ('worse') jumps. The system energy is then gradually lowered, progressively accepting less worse 'moves' (Locatelli 2002). We configured a homogenous-chain simulated annealing heuristic with an energy-dependent Cauchy proposal distribution, a Metropolis-Hastings (Boltzmann) acceptance probability, and a cooling schedule of $\frac{E_0}{k}$, where k = the cooling iteration. At each E , we ran a homogenous Markov Chain for 5,000 improvements, or 15,000 iterations, whichever occurred sooner. We stopped optimisation when $E < 0.50$. For each FSA run, we tuned the per-parameter step size offline to ensure an acceptance rate of 0.25-0.50 for $E = 1$ and tuned E_{max} such that the acceptance rate of worse moves was above 0.60. For each model hypothesis, FSA was conducted five times to ensure that a minimum was identified.

Locatelli, M., 2002. *Simulated annealing algorithms for continuous global optimization, Handbook of global optimization*,

Note S1 Sensitivity analysis of a global versus local calibration of the $\delta^{15}\text{N}$ – N relationship

Method. We conducted an additional sensitivity analysis of our modelling approach to the assumed relation between unitless soil N availability and $\delta^{15}\text{N}$. We consider that the stated global model is most appropriate for our analysis, as the greater geographical, species, and mycorrhizal variability dampens noise, whereas a subset of data for northern areas is limited to Alaska – a temperate boreal region with different Quaternary history and soil development to Yamal – and is more system-specific (i.e., limited to ectomycorrhizal-associated plant species in a tundra environment) thus more vulnerable to site / species specificity. Hobbie et al (1999) measured foliar $\delta^{15}\text{N}$ and soil NO_3^- and NH_4^+ mineralisation rates within sites at Glacier Bay National Park, Alaska, for three ectomycorrhizal-associated species: *Salix spp.*, *Picea sitchensis*, and *Populus trichocarpa*. We fit a relationship for the Hobbie et al (1999) dataset using reduced major axis regression from the *lmodel2* R package (Legendre 2018); the resultant equation was: $\text{N} = (\delta^{15}\text{N} + 10.80) / 11.274$. We assessed the sensitivity of model fits to the global model by comparing the most appropriate models (as specified in **Section 3.4**) to those identified when applying the Alaska-specific equation.

Result. Substituting the global calibration of the $\delta^{15}\text{N}$ – N availability relationship to the Alaskan-specific relationship did not change the importance of N-limitation or plant-soil feedbacks. Akaike weights obtained when substituting the Alaskan $\delta^{15}\text{N}$ – N availability relationship are shown in the below table:

Akaike weights for each shrub and hypothesis for a sensitivity analysis of d15N-nitrogen relationship (wherein global meta-analysis relationship from Craine et al (2009) replaced with function derived from Hobbie et al (1999)).

[illegible]

Asymptotic:										
Saturating	0.00	0.00	0.04	0.00	0.01	0.00	0.00	0.42	0.00	0.00
Saturating + Feedback	0.01	0.24	0.96	0.07	0.36	0.00	0.00	0.00	0.00	0.00
Linear	0.01	0.00	0.00	0.00	0.00	0.00	0.00	0.00	0.00	0.00
Linear + Feedback	0.06	0.74	0.00	0.93	0.06	0.00	0.20	0.19	0.00	0.00
No N Limitation	0.00	0.00	0.00	0.00	0.00	0.00	0.00	0.00	0.00	0.00
Plant-Driven N Cycling	0.00	0.00	0.00	0.00	0.00	0.00	0.00	0.00	0.00	0.00

Akaike weights represented as percentages, to two decimal places. Bold = above 10% support; Red = best supported models

All ten shrubs exhibited N-limited growth irrespective of the included $\delta^{15}\text{N}$ – N relationship. The role of plant-soil feedbacks did not change for nine of ten individuals. A change was observed within the form of N-limitation from linear to saturating form within four individuals' most appropriate models.

Discussion. A switch to saturating N-limitation for a subset of individuals when using the Alaskan $\delta^{15}\text{N}$ – N relationship conforms with our interpretation. The Alaskan model indicates relatively greater N availability at lower $\delta^{15}\text{N}$ compared to the global model; saturation therefore would occur as individuals' abilities to exploit greater levels of N was limited within each growing season.

Hobbie, E.A., Macko, S.A. & Shugart, H.H., 1999. Insights into nitrogen and carbon dynamics of ectomycorrhizal and saprotrophic fungi from isotopic evidence. *Oecologia*, 118(3), pp.353–360.

Legendre, P., 2018. lmodel2: Model II Regression. R package version 1.7-3.